

## A Test of Source-Surface Model Predictions of Heliospheric Current Sheet Inclination

M.E. Burton, E.J. Smith

Jet Propulsion Laboratory

California Institute of Technology

Pasadena, Ca

N.U. Crooker, G.L. Siscoe

Department of Atmospheric Sciences

University of California, Los Angeles

### Abstract

The orientation of the heliospheric current sheet predicted from a source surface model is compared with the orientation determined from minimum variance analysis of ISEE-3 magnetic field data at 1 AU near solar maximum. Of the 37 cases analyzed, 28 have minimum variance normals that lie orthogonal to the predicted Parker spiral direction. For these cases, the correlation coefficient between the predicted and measured inclinations is 0.6. However, for the subset of 14 cases for which transient signatures (either interplanetary shocks or bidirectional electrons) are absent, the agreement in inclinations improves dramatically, with a correlation coefficient of 0.96. These results validate not only the use of the source surface model as a predictor but the previously questioned usefulness of minimum variance analysis across complex sector boundaries. In addition, the results imply that interplanetary dynamics have little effect on current sheet inclination at 1 AU. The dependence of the correlation on transient occurrence suggests that the leading edge of a coronal mass ejection (CME), where transient signatures are detected, disrupts the heliospheric current sheet, but that it reforms between the trailing legs of

the CME. In this way the global structure of the heliosphere, reflected both in the source surface maps and in the interplanetary sector structure, can be maintained even when the CME occurrence rate is high.

## Introduction

The concept of a potential magnetic field model of the corona with a spherical source surface concentric with the sun was introduced by Schatten et al. [1969] and Altschuler and Newkirk [1969]. The model assumes that between the photosphere and the source surface the magnetic field can be described in terms of a scalar potential that satisfies Laplace's equation. The boundary condition at the source surface is that the field is entirely radial. The inner boundary condition is supplied by almost daily observations of the line-of-sight magnetic field made at the Stanford Solar Observatory. Contour maps of the source surface field, which give the orientation of the neutral line, marking the base of the heliospheric current sheet, have been produced by Hoeksema and Scherrer [1986] for the period 1976 to 1985.

Various studies have tested the source surface model using both other solar observations and measurements of the interplanetary magnetic field. Bruno et al. [1984] found good agreement between the shape and location of the model neutral line in 1976 and 1977 and the maximum brightness curves from K-coronameter observations. They also compared source-surface model predictions with the polarity of the interplanetary magnetic field, using observations from IMP 8 and Helios 1 and 2, at distances less than or equal to 1 AU. For each Carrington rotation the ratio between the number of intervals with a given polarity observed at the spacecraft and the number expected was calculated. An agreement of 79% was found. Hoeksema et al. [1983] made a similar comparison during the period 1978- 1982 and found fairly good agreement between the interplanetary magnetic field polarity predicted by the model with that observed near earth. Behannon et al. [1989] compared the model with magnetic

polarity observed by various spacecraft including PVO, Helios, IMP, ISEE-3 and Voyager. Patterns were found to agree 82% of the time between the model and PVO in the inner heliosphere and 61-64% of the time between the model and Voyagers 1 and 2 in the outer heliosphere. Since these studies indicate that at 1 AU the source surface model is a reasonably good predictor of the interplanetary magnetic field polarity, which depends on the shape and location of the heliospheric current sheet, we use it here as a predictor of current sheet inclination.

Application of the minimum variance technique [Sonnerup and Cahill, 1967] to determine the orientation of the heliospheric current sheet in interplanetary space is complicated by sector boundary structure. Typically the magnetic field is highly variable in magnitude and direction, with a number of directional discontinuities, which may represent multiple current sheets [Crooker et al., 1993]. Even seemingly simple sector boundaries commonly found in low-resolution data may consist of a large number of discontinuities when observed in high-resolution. All of these factors complicate both a uniform definition of the sector boundary and selection of the appropriate time interval over which to perform minimum variance analysis. Klein and Burlaga [1980] chose to define the sector boundary as the total region of transition from one polarity state to the other, ignoring the multiple discontinuities. They require that the sector polarity persists for at least two days. On the other hand, Behannon et al. [1981] chose to apply the minimum variance technique to all discontinuities across a sector boundary that separate fields with large angular differences. They found high variability in the inclinations of the discontinuity surfaces, although in azimuth they tend to align with the Parker spiral.

In a case study of a complicated sector boundary crossing, Crooker et al. [1993] found a high degree of variability in orientations of the multiple discontinuities, in agreement with

Behannon et al, [1981]. However, minimum variance analysis across the entire region of frequent discontinuities, following Klein and Burlaga [1980], yielded a normal orthogonal to the Parker spiral and inclined exactly orthogonal to the neutral line on the corresponding source surface map. It is this remarkable coincidence which led to the present study. Accordingly, for the purpose of comparing with source surface predictions, we treat the sector boundary on a global scale and apply our minimum variance analysis across the range of major discontinuities.

Other case studies that compare minimum variance results to neutral line orientations on coronal maps yield mixed results. Behannon et al. [1983] compared minimum variance orientations at Voyager 1 and 2 with coronagraph inclinations. Two cases in the coronagraph data were considered, one vertical and one nearly horizontal. For the vertical case, the orientation from variance analysis of hour averages of the magnetic field data was consistent with the high inclination. But for the horizontal case, minimum variance analysis did not give a low inclination. A similar result was obtained by Villante and Bruno [1982] with Helios 2 observations from early 1976. They found high inclinations with minimum variance analysis when low inclinations characteristic of solar minimum were anticipated. Both Behannon et al. [1983] and Villante and Bruno [1982] attribute their results to highly inclined wrinkles in a current sheet with a low inclination on the global scale, as deduced earlier by Villante et al. [1979] from Helios 2 polarity measurements (see, also, Klein and Burlaga [1980] and Burlaga et al. [1981]). Since our study is confined to data from the launch of ISEE 3 in August, 1978, to February, 1980, we avoid the complications of globally low heliospheric current sheet inclinations during solar minimum.

Our study is the first to compare source-surface model predictions of heliospheric current sheet inclinations with minimum variance determinations from interplanetary data in a systematic

way for a large number of cases. Given the assumptions in the source surface model, the complexity of sector boundary structure, and the uncertainties in the minimum variance technique, a null result would not be surprising. However, our decidedly positive result described below helps put to rest most concerns over the assumptions, complexities, and uncertainties.

## Analysis

### Correlation of model neutral line with interplanetary sector boundaries

From August, 1978, to February, 1980, the source surface model predicts 53 sector boundary crossings at ISEE-3. To locate these in the data we used the ISEE-3 solar wind velocity to map the source surface to the sector boundary. Sector boundaries were provisionally identified by  $180^\circ$  changes in the azimuthal angle of the magnetic field, which tends to lie along the inward ( $135^\circ$ ) or outward ( $315^\circ$ ) Parker spiral direction at 1 AU. Figure 1 shows the hourly averages of this angle over a portion of the interval of this study. To qualify as a correct identification, the dominant polarity of the magnetic field preceding and following the sector boundary was required to persist for a length of time roughly equivalent to that predicted by the model. Of the 53 sector boundary crossings predicted by the model, 38 were unambiguously identified in the magnetic field data at ISEE-3.

### Analysis interval selection criteria

We used the following criteria for determining the appropriate minimum variance analysis interval. A polarity of +1 or -1 was assigned to a five-minute average of the magnetic field if it fell within a cone angle of  $15^\circ$  surrounding the inward or outward spiral directions, respectively. If the magnetic field vector fell outside this cone angle, the polarity was deemed ambiguous and assigned a value of zero. Sector boundaries are characterized by either alternating or ambiguous polarity, where the field does not lie along the spiral direction. The start and stop times of the minimum variance interval were determined by requiring that the entire interval of alternating or ambiguous polarity be included. Minor disruptions in polarity persistence caused by discontinuities shorter than one hour which occurred outside the interval of major polarity changes were not considered to be part of the sector boundary.

An example in Figure 2 illustrates the application of our criteria. The top panel shows the source surface contours during Barrington rotation 1674. The model predicts an intersection with the neutral line on October 31, 1978 (day 304). The solar wind speed of 315 km/sec measured at ISEE-3 upstream of the sector boundary indicates an arrival time at 1 AU on day 310, which is when it is first observed in the data. Panels b, c and d display five minute averages of the field magnitude  $B$ , the latitude angle of the field  $\theta$ , and the azimuthal angle  $\phi$ . The magnetic field polarity in panel e shows that a positive polarity interval ceases on day 310 at 2220 UT, followed by a characteristic alternation between positive, negative and ambiguous polarity after this time until day 311 at 2205 UT. The polarity becomes negative and remains so, with the exception of brief intervals of ambiguous polarity which are not included in the analysis

interval. This entire -24 hour interval, shown by the vertical lines, is considered to be part of the sector boundary and is included in the minimum variance analysis interval.

Using the above criteria on the 38 sector boundaries unambiguously identified at ISEE-3, we applied the minimum variance analysis technique to one-minute averages of the magnetic field, unless the intervals were so long as to make the number of data points intractable ( $>1000$  data points), in which case five-minute averages were used. In addition, we required the eigenvalue ratio  $\lambda_2/\lambda_3$  be greater than two, indicating that the minimum variance ellipsoid was accurate] y determined [Lepping and Burlaga, 1980]. For one sector boundary this requirement was not met, leaving 37 sector boundaries in the final data set.

The sensitivity of the analysis to the interval length is demonstrated in figure 3. Five-minute averages of the x and y components of the magnetic field in geocentric solar ecliptic (GSE) coordinates (where x is toward the sun and z is perpendicular to the ecliptic plane), the field magnitude, the polarity and the azimuthal angle from a sector boundary on days 165-167, 1979, are plotted. Two different analysis intervals are used as denoted, The shorter interval (dashed lines) is approximately 8 hours long and contains the major polarity reversal in the magnetic field, which occurs at  $\sim 0600$  UT. The longer interval (solid lines) contains most of the adjacent discontinuities and is significantly longer ( $>48$  hours). Both intervals are reasonable choices for analysis since both include depressed and variable field magnitude, which characterize sector boundaries. The minimum variance normals in GSE coordinates for the shorter and longer intervals are (.57, .55, .64) and (.59, .36, .72), corresponding to a difference in inclinations of  $100^\circ$ . This example illustrates that a sector boundary with an obviously central polarity change, often treated as a single heliospheric current sheet crossing, yields roughly the same inclination when treated as a thick sector boundary.



### Calculation of source surface normal

The orientation of the predicted normals to the heliospheric current sheet were determined graphically from the contour maps of the source surface field [Hocksema and Scherrer, 1986]. In GSE coordinates the normal vector on the source surface plots lies in the  $yz$  plane. We propagate the normal vector outward to the spacecraft along the Parker spiral direction by rotating it about the  $z$ -axis through the angle  $Y' = \tan^{-1}(\omega r / v)$ , where  $v$  is the measured solar wind velocity and  $\omega$  is the sun's rotation rate. Thus for a comparison with the ISEE-3 data, all model normals lie orthogonal to the Parker spiral.

### Results

Figure 4 shows the distribution of the angular difference between the normal to the source surface model current sheet and the normal determined by minimum variance analysis for all 37 sector boundaries analyzed. Since the comparison is between two vectors in three-dimensional space, the distribution is normalized by solid angle. The result is that more than 80% of the cases fall within the  $0$ - $20^\circ$  bin.

Previous studies show that normals to the heliospheric current sheet tend to be oriented along the direction perpendicular to the Parker spiral [Thomas and Smith, 1981]. This is also true for our data set. Figure 5 shows the distribution of the difference between the angle orthogonal to  $\Psi$  and the azimuthal angle of the minimum variance normal. The median value is  $11.5^\circ$ , and 28 of the 37 cases fall within  $20^\circ$  of the orthospiral direction. Thus the good

agreement in Figure 4 to a large extent reflects the tendency for the current sheet to align with the Parker spiral. Since the main goal is to test for agreement between the predicted and measured inclination angle,  $I = \cos^{-1} \hat{n} \cdot \mathbf{z}$ , where  $\hat{n}$  is the current sheet normal, we use for further analysis only those cases which align with the Parker spiral. This effectively separates azimuthal from inclination angle agreement and reduces the comparison to two dimensions.

Figure 6 shows the distribution of the difference in inclinations for the 28 cases with normals within  $20^\circ$  of the orthospiral direction. The median value is  $13^\circ$ , and 15 of the 28 cases lie within the  $0$ - $15^\circ$  bin. A scatterplot of the 28 predicted and measured inclinations is shown in Figure 7; the correlation coefficient is 0.6. To test for the effect of CME passage on inclination angle agreement, we separate cases with and without transient signatures which are common at sector boundaries [Crooker et al., 1993], as Figure 1 demonstrates. Observations of bidirectional electrons (BDEs) are shown by the shaded regions. Interplanetary shocks identified by signatures in the magnetic field are indicated by arrows. For 14 of the 28 cases plotted in Figure 7, no transient signatures were found. The correlation coefficient for these cases (large dots) is 0.96. In the absence of transients, agreement between the predicted and measured inclinations is remarkably good,

In figure 8 the distributions of predicted and measured inclinations are shown in separate histograms to test for evidence of current sheet steepening by interplanetary stream interactions. The average predicted inclination is  $59^\circ$  and the average measured inclination is  $61^\circ$ . These values are consistent with no steepening between the source surface at 2.5 Rs and 1 AU.

An estimate of the average sector boundary thickness can be made from the time intervals of the sector boundary crossings determined by the criteria discussed above. Figure 9 shows the distribution of the crossing intervals in hours. The average value of all cases is 26.4 hours. For

a solar wind speed of 400 km/s, this corresponds to a thickness of 0.25 AU. The large peak in the 0-10 hour bin reflects the high occurrence of sector boundaries dominated by a single polarity reversal. Three cases were omitted because of data gaps. In four cases in figure 9 the polarity reverses abruptly between two consecutive five-minute averages. In view of our definition that the sector boundary includes the entire region of disturbed or ambiguous polarity, it is clear that sector boundaries with transient signatures should be thicker structures. This is evident in panels b and c of Figure 9, for cases with and without transient signatures. The respective average values are 38.1 and 12.5 hours.

## Discussion

This paper provides the first extensive test of the source surface model as a predictor of heliospheric current sheet inclination at 1 AU. The results show that the predictions match nearly exactly ( $r = 0.96$ ) the inclinations derived from minimum variance analysis across sector boundaries in the absence of transient signatures. The excellent agreement implies that interplanetary dynamical processes between the sun and 1 AU do little to erase the solar imprint on heliospheric structure.

It may be considered surprising that in this period approaching solar maximum, when the heliosphere is filling with CMES, the source surface model can predict inclinations at all. The model assumes that fields beyond the source surface are open and lie along the Parker spiral, while closed fields with large components orthogonal to the Parker spiral are associated with CMEs. Figure 10 offers a possible interpretation of the result. It illustrates two successive CMEs which arose from a helmet streamer at the base of the streamer belt. Each creates only a

brief disruption in the current sheet at the leading edge as it passes through the streamer belt corridor [Crooker et al., 1993], Anti parallel fields forming the legs of the CME require re-formation of the current sheet behind the leading edge. The fields there may be closed, but they are radial, as in the source surface model.

Our analysis shows that transient signatures were encountered during half of the sector boundary crossings and that in these cases agreement between the predicted and measured inclinations declined ( $r = 0.3$ ). In terms of Figure 10, this means that the chances of being immersed in the leading edge of a CME at 1 AU while crossing the sector boundary were one in two, so that the streamer belt was filled with a train of CMEs, consistent with the high CME rate near solar maximum [Webb, 1991]. We interpret the reduced correlation coefficient as a reflection of cases where ISEE-3 passed through gap in the current sheet in the leading edge of the CME.

In the interpretation offered here, heliospheric current sheet inclinations and disruptions at 1 AU near solar maximum are both controlled by their solar source rather than interplanetary dynamics. The inclinations are determined by neutral line inclination on source surface maps, and the disruptions are caused by passage of the leading edge of CMEs.

## Conclusions

At 1 AU near solar maximum,

1. The source surface model of coronal fields is an excellent predictor of global heliospheric current sheet inclination, in the absence of transient signatures there.

2. Interplanetary dynamics have no measurable effect on global heliospheric current sheet inclination.

3. Heliospheric sector structure can be maintained in the presence of frequent coronal mass ejections.

### Acknowledgements

This paper represents work done at the Jet Propulsion Laboratory, California Institute of Technology under contract NAS 7-918 and its subcontract 959485 from JPL to UCLA.

## References

- Altschuler, M.D. and G. Newkirk Jr., Magnetic fields and the structure of the solar corona, *Solar Physics*, 9, 131, 1969.
- Behannon, K. W., F.M. Neubauer and H. Barnstorf, Fine-scale characteristics of interplanetary sector boundaries, *J. Geophys. Res.*, 86, 3273, 1981.
- Behannon, K.W., L.F. Burlaga, and A.J. Hundhausen, A comparison of coronal and interplanetary current sheet inclinations, *J. Geophys. Res.*, 88, 7837, 1983.
- Behannon, K. W., L.F. Burlaga, J. T'. Hoeksema and L.W. Klein, Spatial variation and evolution of heliospheric sector structure, *J. Geophys. Res.*, 94, 1245, 1989.
- Bruno, R., L.F. Burlaga, and A.J. Hundhausen, K-coronameter observations and potential field model comparison in 1976- 1977, *J. Geophys. Res.*, 89, 5381, 1984.
- Crooker, N. U., G.L. Siscoe, S. Shodhan, D.F. Webb, J.T. Gosling, and E.J. Smith, Multiple heliospheric current sheets and coronal streamer belt dynamics, *JGR*, 1983, in press.
- Hoeksema, J. T., J.M. Wilcox and P.H. Scherrer, The structure of the heliospheric current sheet: 1978-1982, *J. Geophys. Res.*, 88, 9910, 1983.
- Hoeksema, J.T. and P.H. Scherrer, The Solar Magnetic Field -- 1976 through 1985, Rep UAG-94, World Data Cent. A for Sol. -Terr Phys., Natl. Oceanic and Atmos. Admin., Boulder, Colo., 1986.
- Klein, L. and L.F. Burlaga, Interplanetary sector boundaries 1971-1973, *J. Geophys. Res.*, 85, 2269, 1980.
- Lepping, R.P. and K.W. Behannon, Magnetic field directional discontinuities, 1, minimum variance errors, *J. Geophys. Res.*, 85, 4695, 1980.
- Schatten, K., J.M. Wilcox, and N.F. Ness, A model of interplanetary and coronal magnetic fields, *Solar Phys.*, 6, 442, 1969.
- Smith, E. J., J.A. Slavin and B.T. Thomas, The heliospheric current sheet: 3-dimensional structure and solar cycle changes, in *Proceedings of the ESLAB Symposium on the Three Dimensional Structure of the Heliosphere*, p. 267, D. Reidel, Hingham, Mass., 1986.
- Sonnerup, B. U. O., and L.J. Cahill, Magnetopause structure and attitude from Explorer 12 observations, *J. Geophys. Res.*, 72, 171, 1967.
- Thomas, B.T. and E.J. Smith, The structure and dynamics of the heliospheric current sheet, *J. Geophys. Res.*, 86, 11105, 1981.

Villante, U., B. Bruno, F. Mariani, L. F. Burlaga, and N.F. Ness, The shape and location of the sector boundary surface in the inner solar system, J. Geophys. Res., 84, 6641, 1979,

Villante, U. and R. Bruno, Structure of current sheets in the sector boundaries: Helios 2 observations during early 1976, J. Geophys. Res., 87, 607, 1982.



## Figure Captions

figure 1. Hourly averages of the azimuthal angle of the magnetic field for a portion of the interval of our study. Sector boundaries are characterized by a transition in the azimuthal angle from the Parker spiral direction at 1 AU for toward and away sectors, 315 and 135°. Signatures of transients, both bidirectional electrons and interplanetary shocks which are shown on the figure, tend to be preferentially located at sector boundaries.

figure 2. Sector boundary from Barrington rotation 1674, November, 1978. Panel a shows the source surface contour plot. The horizontal line shows the intersection with the spacecraft latitude. Panels b, c and d are five minute averages of the field magnitude, latitude and azimuthal angles of the field. Panel e is a time series of five minute values of the polarity of the magnetic field as described in the text. The interval chosen as the minimum variance analysis interval is shown by the vertical lines.

figure 3. Sector boundary from days 164-167 (0800 UT), 1979. Five minute averages of the x and y components, the field magnitude, polarity and azimuthal angle of the field are shown. Two sample intervals are shown by the dashed and solid lines,

figure 4. The distribution of the angular difference between the model normal and the minimum variance normal in 3 dimensions. The distribution has been normalized by solid angle.

figure 5, The distribution of the angle between the direction orthogonal to the Parker spiral and the azimuthal angle of the minimum variance normal. Twenty-eight cases lie within twenty degrees of the *orthospiral* direction.

figure 6. The distribution of the angular difference in inclinations between the model normal and the minimum variance normal for the twenty-eight cases which lie within twenty degrees of the *orthospiral* direction.

figure 7. A scatterplot of the model inclination versus the minimum variance inclination. The correlation coefficient for all twenty-eight cases is 0.6 and for the fourteen cases for which no transient signatures are observed the correlation coefficient is 0.96.

figure 8, The distribution of the model inclination (panel a) and the minimum variance inclination (panel b) for the subset of twenty-eight cases oriented along the Parker spiral direction. For this figure the values of the inclinations are folded over into one quadrant so that all values lie within zero and ninety degrees.

figure 9. Distribution of sector boundary crossing times, in hours using the sector boundary definition given in the text. The top panel includes all cases. The middle panel are cases where transients were observed. The bottom panel are cases without transient signatures.

figure 10. Schematic depicting disruption of the current sheet structure by passage of a CME and reformation after its passage.

# ISEE-3 Magnetic Field 1978-79

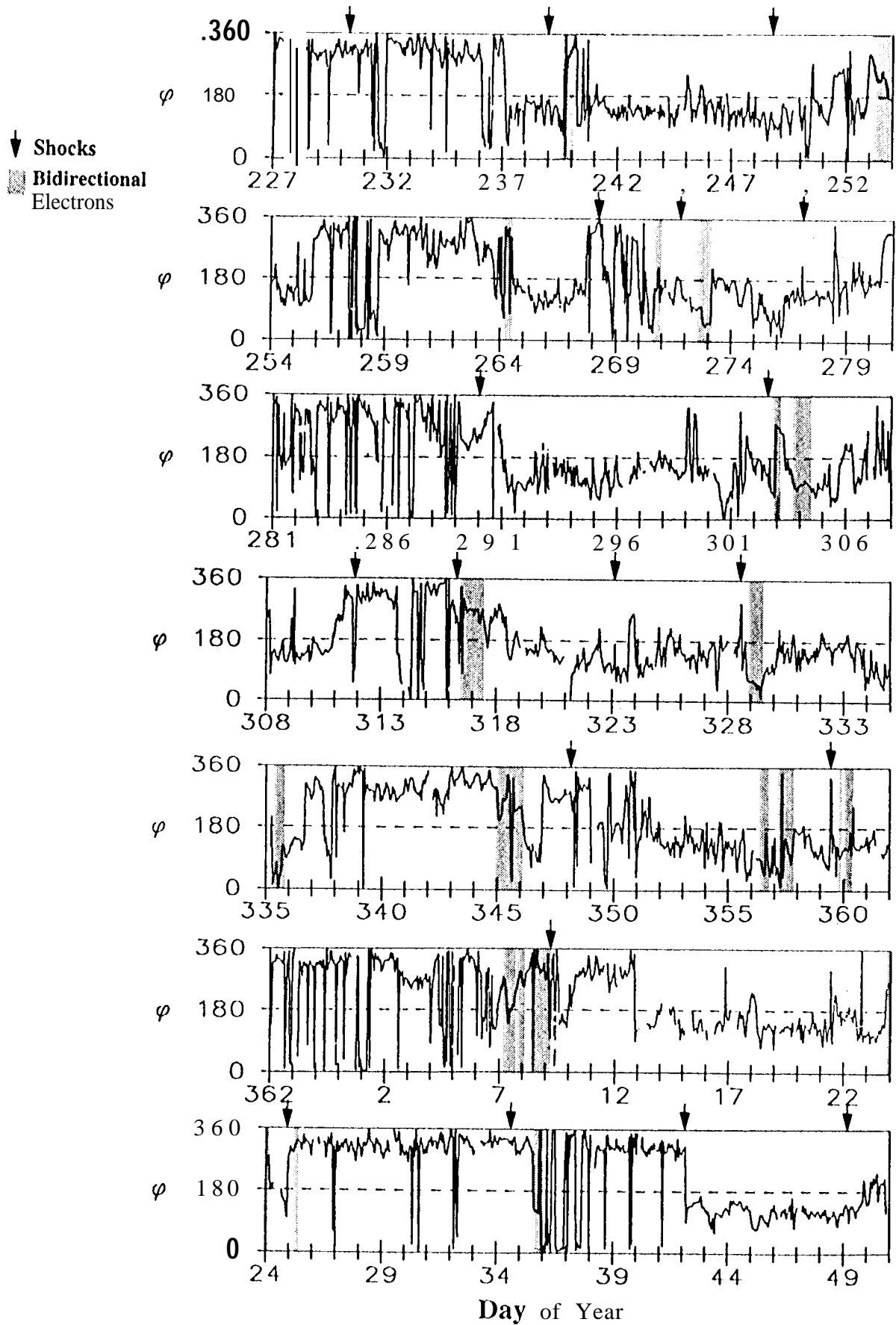


figure 1

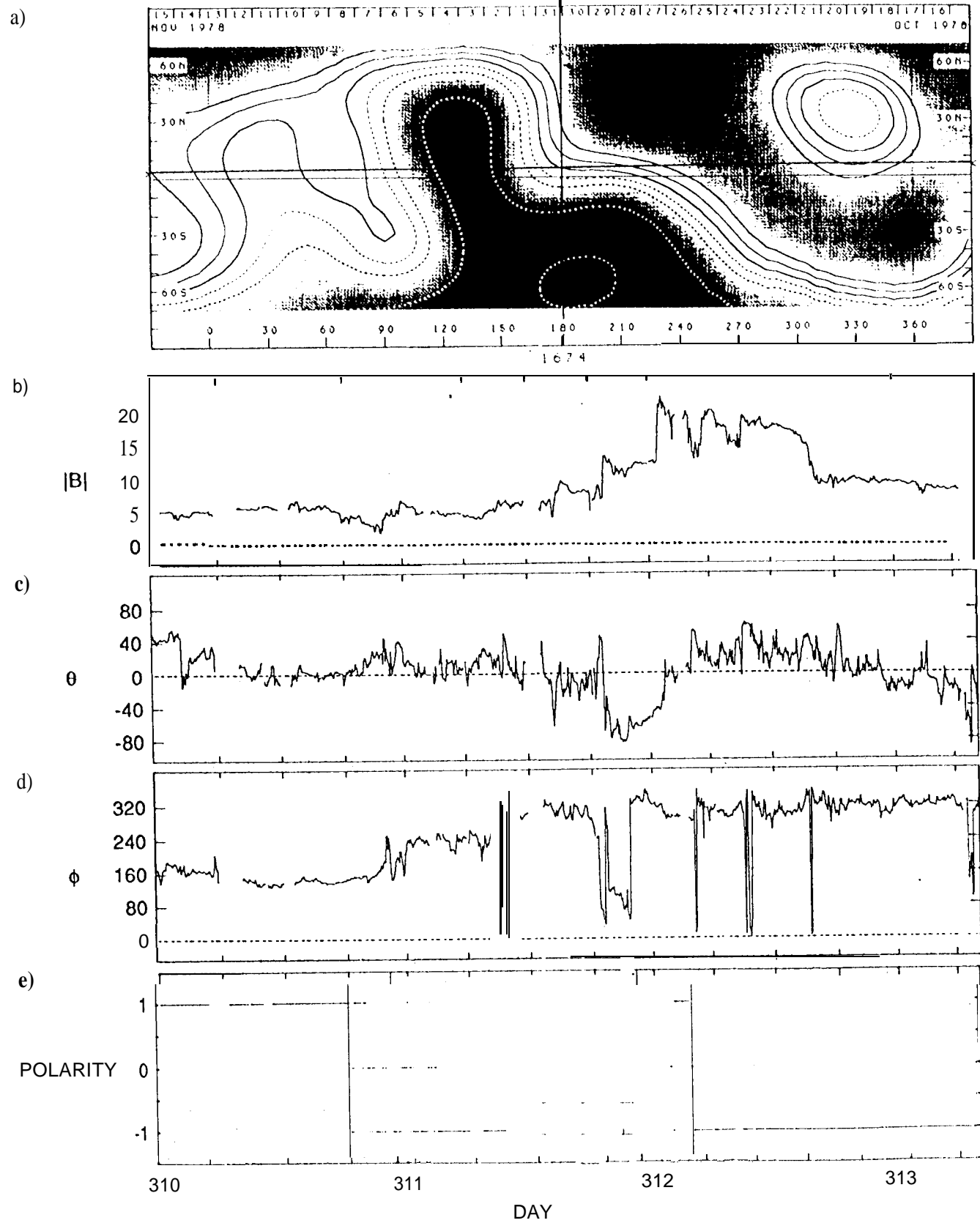


figure 2

ISEE-3 MAGNETIC FIELD  
5-MINUTE AVERAGES  
DAY 164-167 (0800 UT)

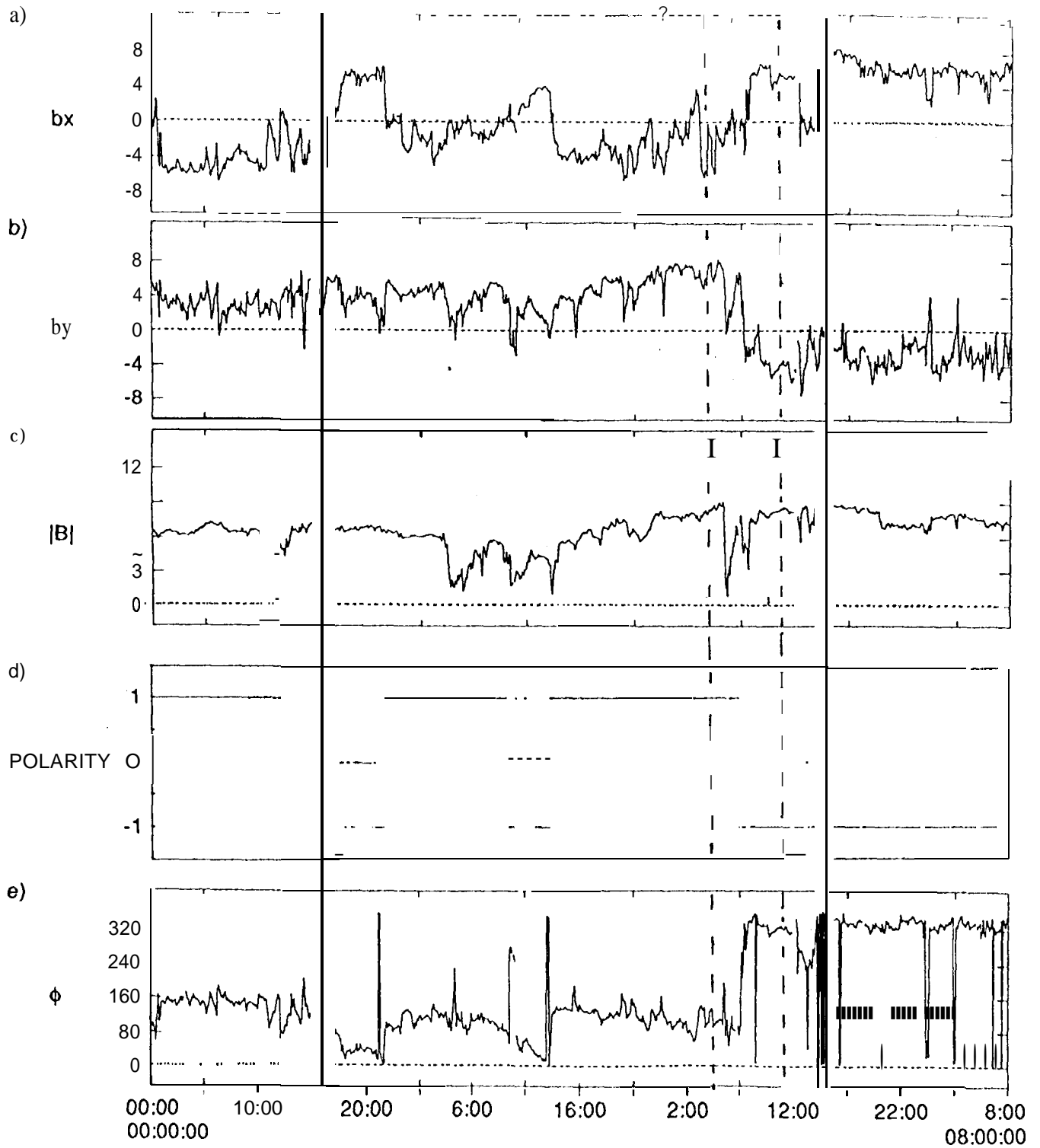


figure 3

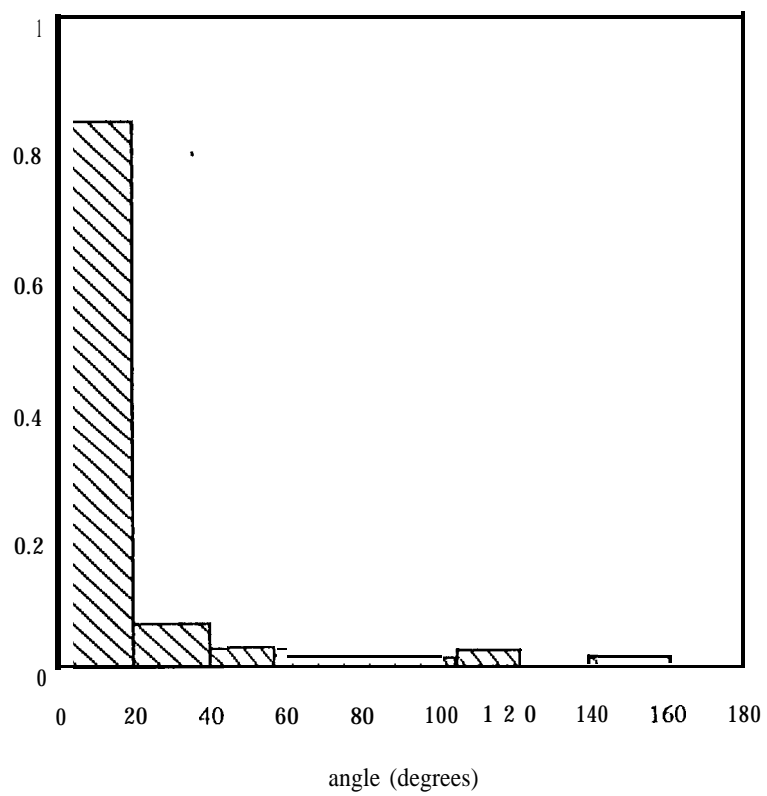
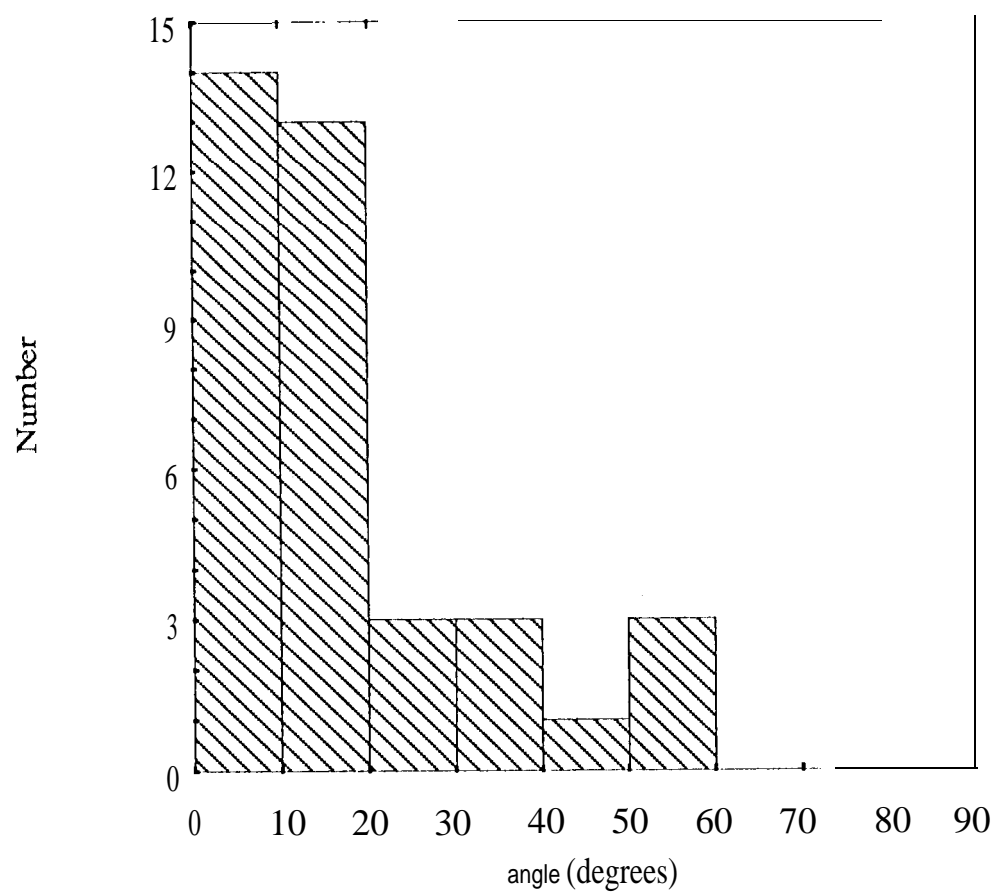


figure 4



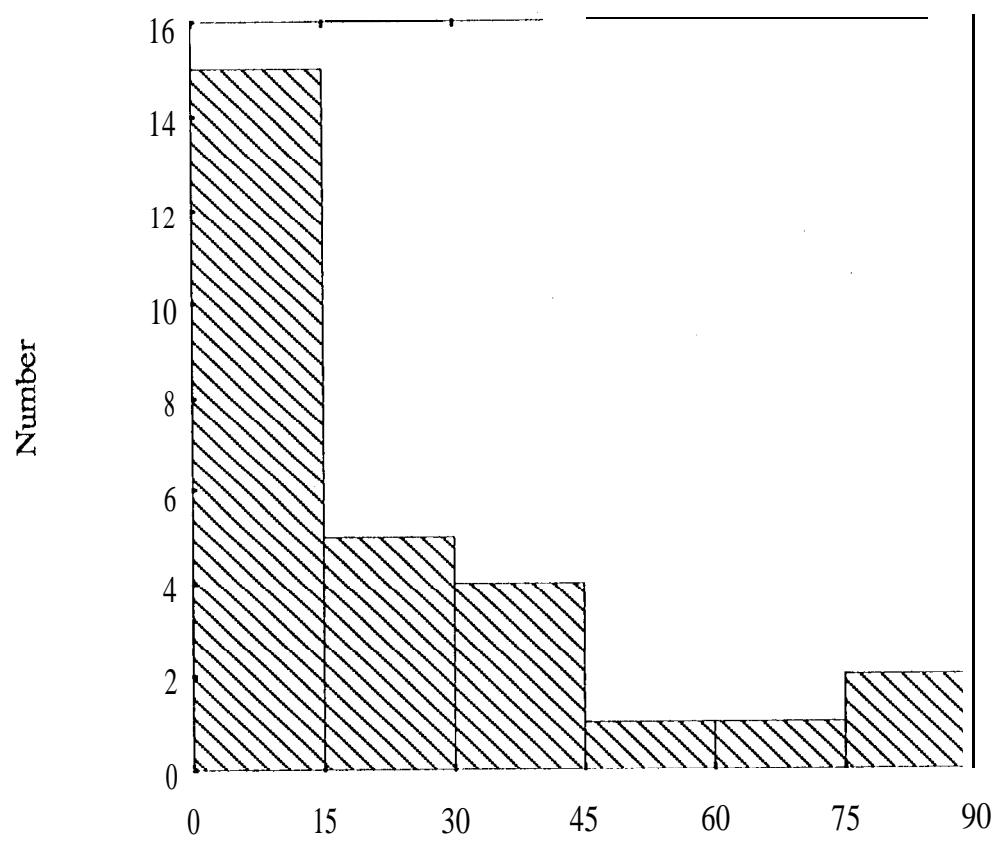


figure 6



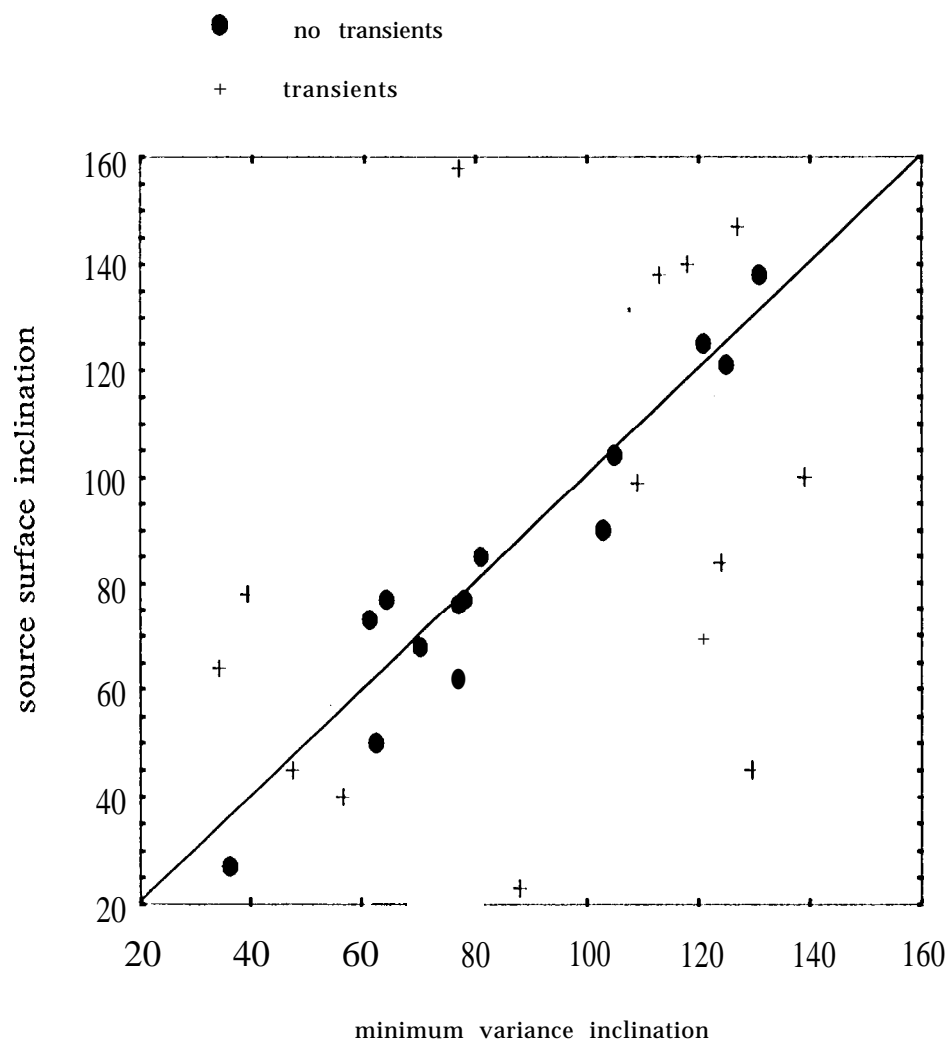


figure 7

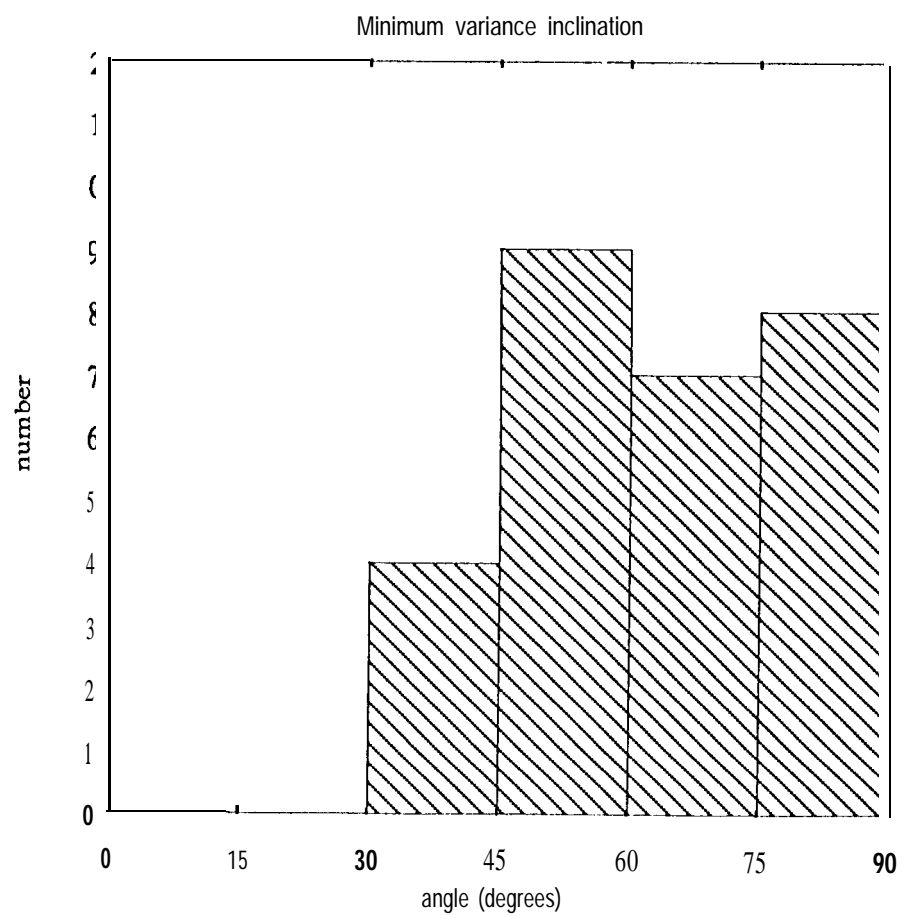
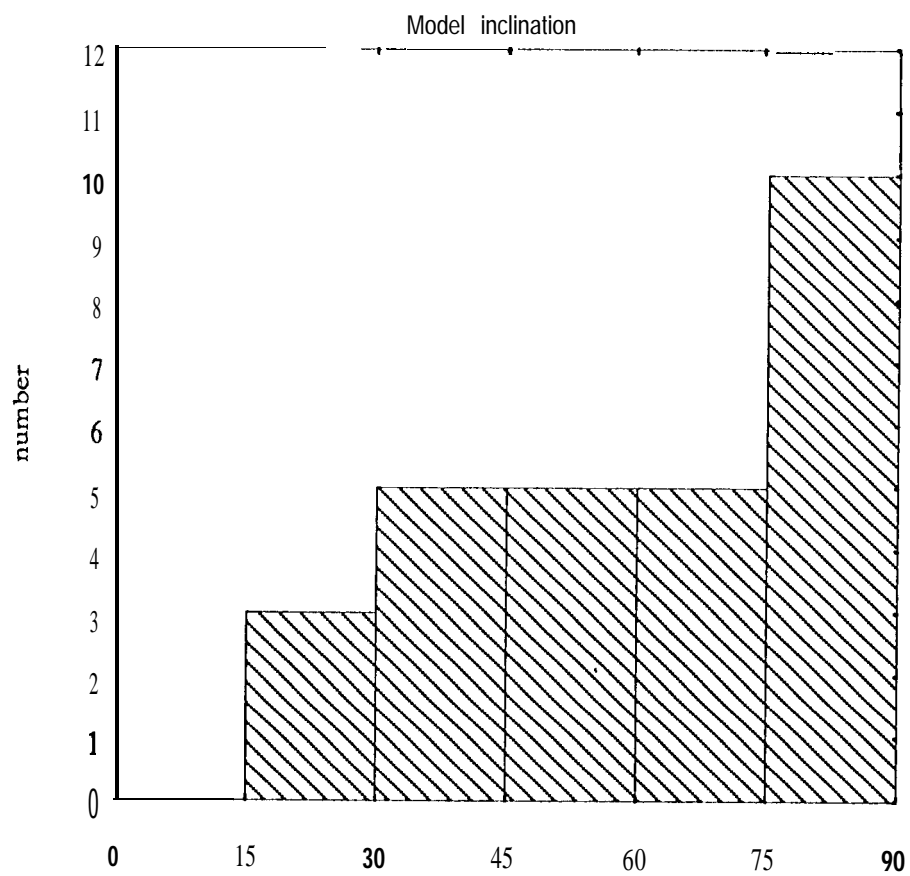


figure 8

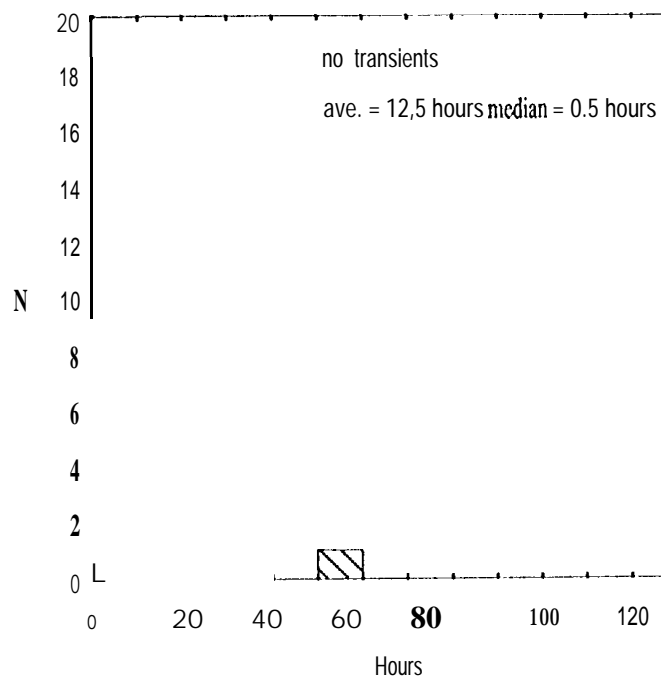
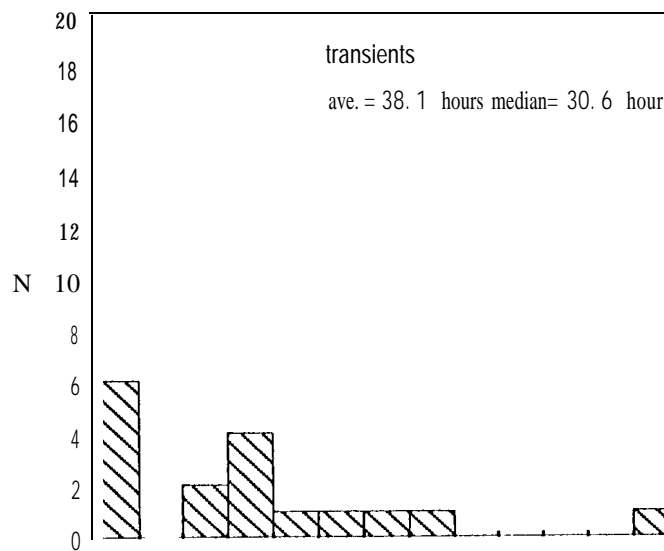
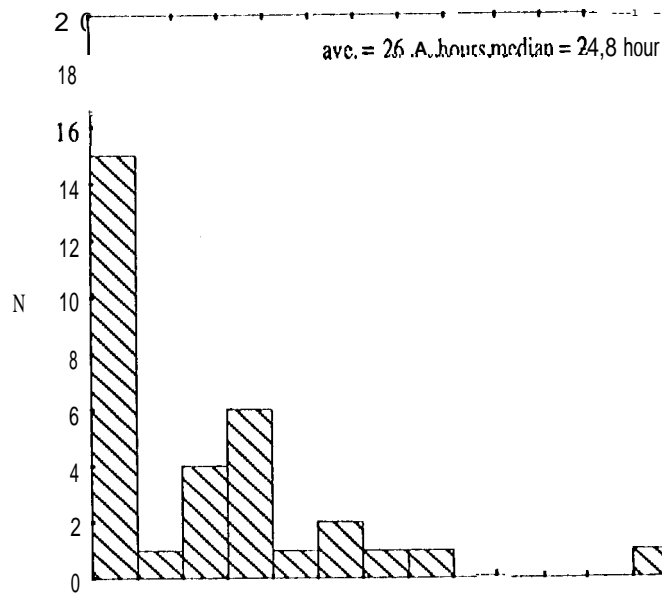


figure 9

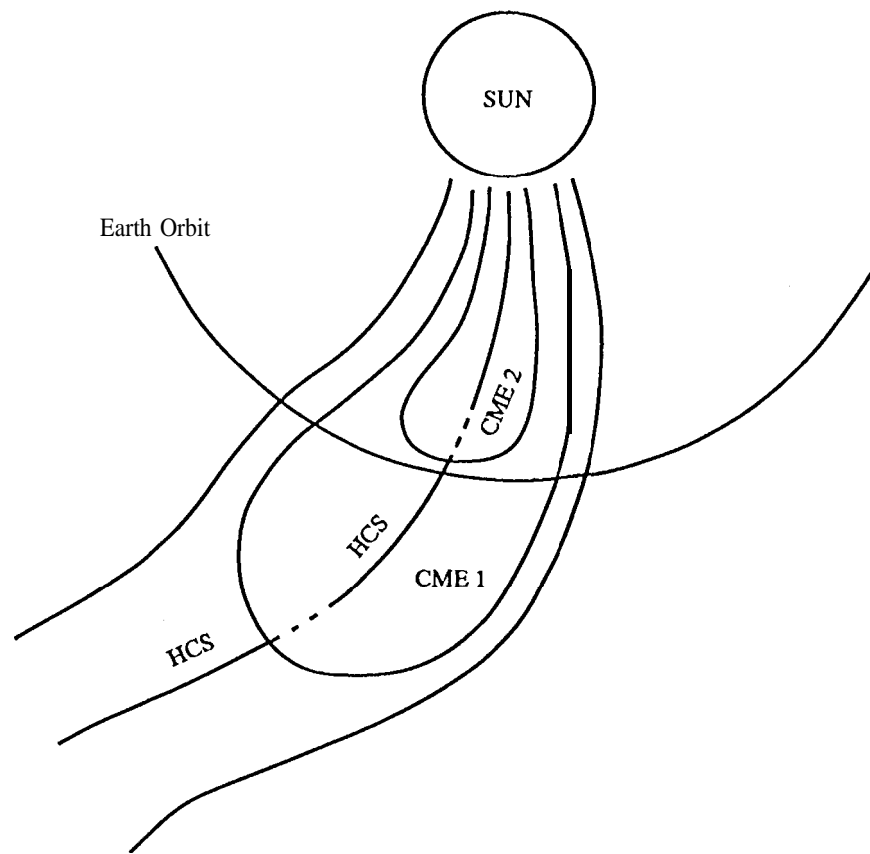


figure 10

Acknowledgements

This paper represents work done at the Jet Propulsion Laboratory, California Institute of Technology under contract NAS 7-918 and its subcontract 959485 from JPL to UCLA.